Proceedings of ENCIT 2012

14th Brazilian Congress of Thermal Sciences and Engineering
November 18-22, 2012, Rio de Janeiro, RJ, Brazil

NUMERICAL SIMULATION OF HEAT TRANSFER IN TWO-PHASE SLUG FLOW USING A SLUG TRACKING METHOD

César D. Perea M., cesar.perea.medina@gmail.com
Carlos L. Bassani, carloslbassani@hotmail.com
Cristiane Cozin, criscozin@yahoo.com.br
Silvio L. M. Junqueira, silvio@utfpr.edu.br
Rigoberto E. M. Morales, rmorales@utfpr.edu.br
LACIT/PPGEM/UTFPR, Av. Sete de Setembro 3165, CEP. 80230-901, Curitiba-PR-Brasil

Abstract. *In the present work, numerical simulation of heat transfer in non-boiling two-phase slug flow is developed for horizontal pipes. Slug flow pattern is characterized by the alternate succession of two structures: an aerated liquid slug and an elongated gas bubble, which constitute a unit cell. This concept is used by the slug tracking models in order to develop a lagrangian model in transient regime, capable of predicting accurately the flow behavior with low computational time. However, slug tracking models are generally developed to predict just the hydrodynamic parameters, ignoring heat transfer. Present work couples the heat transfer governing equations with the slug tracking model through energy balances in deformable and mobile control volumes using the Reynolds transport theorem in its integral form. In addition, a new expression for the calculation of the two-phase heat transfer coefficient is proposed. Numerical results are compared with data from the literature, obtaining good agreement.*

Keywords*: two-phase flow, intermittent flow, convection, heat transfer*

1. INTRODUCTION

The slug flow pattern occurs over a wide range of gas and liquid flow rates. It is characterized by the alternate succession of two structures: a liquid slug and an elongated bubble, which constitute a unit cell. Each of the components of the unit cell has its characteristics changed along the time and space. Accurate prediction of the intermittent flow characteristics is necessary to design the facilities dealing with this type of flow. Therefore, the development of reliable mathematical models for the simulation of slug flow has been a topic of research in the last decades.

The transient nature of slug flow can be modeled through different approaches. One of them is the slug tracking model, which has proved to be capable of predicting accurately the intermittency of slug flow (Nydal, 1995 and Rodrigues, 2009). A slug tracking model performs the mass and momentum balance equations in deformable control volumes from a frame of reference moving with the unit cell. This type of model uses the integral form of the conservation equations; therefore it considers an average value for each control volume which results in a lower computational time.

The early works using slug tracking models just simulated the movement of the bubbles by displacing the whole unit cell with the bubble translational velocity (Barnea e Taitel, 1993). Recently, Rodrigues (2009) presented a slug tracking model that considers the expansion of the gas bubble due to gas compressibility and aerated slugs. This model performs the balance equations for separated liquid slug, liquid film and elongated bubble resulting in two differential equations: one from the mass and other for the momentum balance. However, Rodrigues' slug tracking model is limited to study the hydrodynamics of the flow, neglecting the heat transfer effects.

The study of the heat transfer in slug flow is a matter of importance as it has many industrial applications. One of them is the oil transfer in long production lines, where the pipes are exposed to harsh external conditions. This interaction causes heat exchanges between the two-phase mixture and the surrounding environment. As a result, the temperature of the fluids will vary along the pipeline producing changes in the in-situ properties of the fluids like the density and the liquid viscosity, which are directly related to the pressure drop. In addition, wax deposition or hydrates formation can occur, as these processes depend on the thermodynamic equilibrium.

The studies of heat transfer in two-phase flow mainly concerns about the evaluation of the two-phase convective coefficient. Some authors developed correlations without regarding the flow pattern. Shah (1981), for instance, considered the liquid as the main contributor and a minor influence of the gas through its superficial velocity. Some authors developed models exclusively for intermittent flow such as Hetsroni et al. (1998) and França et al. (2009). Hetsroni et al. (1998) determined that the main parameters that affect heat transfer are the superficial liquid velocity, the bubble length, the bubble translational velocity and the frequency. França et al. (2008) modeled the forced convection through a time averaging process in the unit cell. Kim and Ghajar (2006) evidenced the importance of the wetted perimeter for the estimation of this coefficient and proposed a correlation based on a flow pattern factor.

Despite the interest that authors have shown in this matter throughout, few studies exists that evaluate heat transfer of non-boiling slug flow through energy balance. In addition, two-phase flow heat transfer approaches are limited to calculate the heat transfer coefficient, not considering temperature simulation. In that context, the objective of the present work is to develop a heat transfer model using the slug tracking approach. Heat transfer governing equations are coupled with the Rodrigues (2009) slug tracking model in order to calculate the hydrodynamic and thermal characteristics of the two-phase slug flow along a pipe. Present work considers the deformation of the gas bubble due to pressure and temperature changes. Numerical simulations are performed and compared with data from the literature, obtaining good agreement.

2. HYDRODYNAMIC MODEL

In this section, the slug tracking model presented by Rodrigues (2009) is modified by adding the heat transfer effects. Slug tracking model considers the bubble and liquid slug regions as separated elements that propagates along the pipe. The model results in two differential equations where the variables to be determined are: the liquid slug velocity and the gas bubble pressure. In order to simplify, some hypotheses are assumed: the state of both phases are far from the saturation region so liquid is incompressible and the gas is ideal, negligible forces in the gas bubble, no axial variation of the pressure inside each bubble, liquid holdup in the slug R_{LS} and void fraction in the film R_{LB} are constant with time.

The mathematical one-dimensional model consists on an integral analysis of the mass and momentum balance equations, applied to each component of the unit cell. Figure 1, presents the j^{th} unit cell, with coordinates x_j e y_j that represent the front of the slug and the bubble, respectively. Also, Figure 1: shows the bubble and liquid slug length. L_{Bj} and L_{Sj}, the mean liquid velocity in the film U_{LBj}, the mean dispersed bubble velocity in the slug U_{GSj} and the bubble translational velocity U_{Tj}.

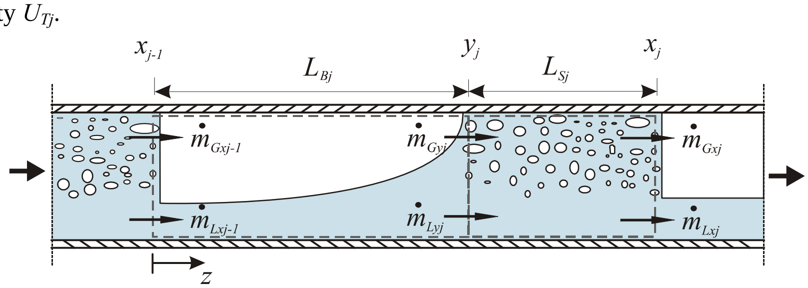

Figure 1: Slug tracking control volumes.

Rodrigues (2009) performs separated mass balances for the slug and the bubble and then couples the resulting equations in one that represents the mass balance for the entire unit cell. As this resulting equation just considers the deformation of the bubble due to pressure drop, it should be modified in order to consider the temperature influence as well. Thus, the overall mass balance for a unit cell with heat transfer is written as:

$$U_{LSj-1} - U_{LSj} = \left(\frac{1-R_{LSj}}{R_{LSj}}\right)U_{DSj} - \left(\frac{1-R_{LSj-1}}{R_{LSj-1}}\right)U_{DSj-1} + \left(\frac{1}{P_{GBj}}\frac{dP_{GBj}}{dt} - \frac{1}{T_{GBj}}\frac{dT_{GBj}}{dt}\right)\times$$
$$\times\left[L_{Bj}\left(1-R_{LBj}\right) + \frac{L_{Sj}}{2}\left(1-R_{LSj}\right) + \frac{L_{Sj-1}}{2}\left(1-R_{LSj-1}\right)\frac{\rho_{GBj}}{\rho_{GBj-1}}\right] \quad (1)$$

In Eq. (1) the difference between the slug velocities in two adjacent unit cells (j and j-1) is related to the gas compressibility of the j^{th} gas bubble and the mass fluxes crossing the control surfaces x_{j-1} and y_j. The expansion (or compression) occurs due to the variation of the geometric characteristics on the unit cell along the space, the pressure decrease and the temperature variations along the time.

Momentum balance is performed in the liquid slug. The pressures obtained from this balance are evaluated on the slug surfaces. However, Rodrigues (2009) expresses them as a function of the bubble pressures by applying balance equations in the positions y_j and x_j. At position y_j, pressure is constant in the slug and bubble due to the smooth shape of the bubble front. At x_j, a stationary balance shows that the pressure drop is caused by the friction and gravitation term on the liquid film. Considering the conditions above, the momentum balance in the liquid slug is:

$$P_{GBj} - P_{GBj+1} = \tau_{LSj}\frac{S_{LSj}L_{Sj}}{A} + \tau_{LBj+1}\frac{S_{LBj+1}L_{Bj+1}}{A} + g\rho_L Sen\beta\left(R_{LSj}L_{Sj} + R_{LBj+1}L_{Bj+1}\right) + \rho_L R_{LSj}L_{LSj}\frac{dU_{LSj}}{dt} \quad (2)$$

where τ_{LBj+1} is the shear stress of the liquid film, S_{LBj+1} is the liquid wetted perimeter in the film, A is the area of cross-section of the pipe.

Equations (1) and (2) constitute the coupled system of the slug tracking model formed by two differential equations. In order to solve numerically, the system is discretized using the semi-implicit Crank-Nicholson scheme (Patankar, 1980).For the shear stress, the Fanning friction factor is used. The discretized form of Eqs. (1) and (2) become:

$$\left[U_{LSj-1}^{N}-U_{LSj}^{N}\right]-\frac{2}{\Delta t P_{GBj}^{O}}\left(L_{Bj}R_{GBj}+\frac{L_{Sj}}{2}R_{GSj}+\frac{L_{Sj-1}}{2}R_{GSj-1}\frac{\rho_{GBj}^{O}}{\rho_{GBj-1}^{O}}\right)P_{GBj}^{N}=\left[U_{LSj}^{O}-U_{LSj-1}^{O}\right]$$
$$-\frac{2}{\Delta t}\left(1-\frac{T_{GBj}^{O}-T_{GBj}^{OO}}{T_{GBj}^{O}}\right)\left(L_{Bj}R_{GBj}+\frac{L_{Sj}}{2}R_{GSj}+\frac{L_{Sj-1}}{2}R_{GSj-1}\frac{\rho_{GBj}^{O}}{\rho_{GBj-1}^{O}}\right)+2\Delta U_{DSj} \quad (3)$$

$$\left[P_{GBj+1}^{*N}-P_{GBj}^{*N}\right]+\left(\frac{2R_{LSj}L_{Sj}}{\Delta t}+4f_{LSj}\frac{L_{Sj}}{D}U_{LSj}^{O}\right)U_{LSj}^{N}=\left[P_{GBj}^{*O}-P_{GBj+1}^{*O}\right]+2R_{LSj}L_{Sj}\frac{U_{LSj}^{O}}{\Delta t}-\frac{2}{\rho_L}\left(\Delta P_{Sj+1}+\Delta P_{Gj}\right) \quad (4)$$

where Δt is the time step, $\Delta U_{DSj} = (1-R_{LSj})U_{DSj}/R_{LSj} - (1-R_{LSj-1})U_{DSj-1}/R_{LSj-1}$, $\Delta P_{Gj} = \rho_L g Sen\beta(R_{LSj}L_{Sj} + R_{LBj+1}L_{Bj+1})$, $\Delta P_{Sj+1} = 2f_{LBj+1}L_{Bj+1}\rho_L S_{LBj+1}U^2_{LBj+1}/\pi D^2$. The super-indexes N and O refer to the parameters evaluated in the new and old instant respectively.

3. HEAT TRANSFER MODEL

In order to obtain the heat transfer governing equations, energy balance is applied in the control volumes corresponding to the unit cell, which are specified in Figure 1:. The energy balance equation in the integral form is given by the Reynolds transport theorem and the first law of thermodynamics:

$$\dot{Q}-\dot{W}_{visc}=\frac{d}{dt}\int_{\forall C}\left(\hat{u}+e_k+e_p\right)\rho d\forall+\int_{SC}\left(i+e_k+e_p\right)\rho V_r\cdot dA \quad (5)$$

where $\dot{Q}$ is the heat rate provided to the control volume, $\dot{W}_{visc}$ is the energy loss due to viscous dissipation, $\hat{u}$ is the internal energy, e_k is the kinetic energy, e_p is the potential energy, i is the specific enthalpy, V_r the relative velocity in the control surface and A the cross section area.

Some considerations must be made: viscous dissipation is negligible, kinetic energy is little compared to the internal energy and potential energy is zero if the reference is aligned with the horizontal pipe. As it is a one-dimensional problem, the heat rate provided to the control volume is the energy exchange with the wall so that, the heat rate can be calculated using the Newton's law of cooling.

Energy balance equations must be applied in each control volume in the unit cell: liquid slug, liquid film and elongated bubble. It should be clarified that the dispersed bubbles in the liquid slug have the same temperature as the liquid surround them, so it is not necessary to apply the energy equation to them. Thus, the energy balance equation is applied to the liquid slug, obtaining:

$$\overline{h_{LSj}^{G}}S_{LSj}L_{Sj}\left(T_{wLSj}-T_{LSj}\right)=\rho_L A R_{LSj}\frac{d}{dt}\left(\hat{u}_{LSj}L_{Sj}\right)+\dot{m}_{Lxj}\,i_{Lxj}-\dot{m}_{Lyj}\,i_{Lyj} \quad (6)$$

where $\dot{m}_{Lxj} = \rho_L A R_{LSj}|U_{LSj} - dx_j/dt|$, $\dot{m}_{Lyj} = \rho_L A R_{LSj}|U_{LSj} - dy_j/dt|$, $\overline{h^G}$ is the global heat transfer coefficient of the liquid slug, T_w is the wall temperature, T is the fluid mean temperature dx_j/dt is the velocity of displacement of the back of the bubble, dy_j/dt is the velocity of the front of the bubble. Indexes LSj, LBj and GBj refer to the slug, film and elongated bubble of the j- unit cell respectively.

The same concept is used for the liquid film and the elongated bubble:

$$\overline{h_{LBj}^{G}}S_{LBj}L_{Bj}\left(T_{wLBj}-T_{LBj}\right)+h_{ij}S_{ij}L_{Bj}\left(T_{GBj}-T_{LBj}\right)=\rho_L A R_{LBj}\frac{d}{dt}\left(\hat{u}_{LBj}L_{Bj}\right)+\dot{m}_{Lyj}\,i_{Lyj}-\dot{m}_{Lxj-1}\,i_{Lxj-1} \quad (7)$$

$$\overline{h_{GBj}^{G}}S_{GBj}L_{Bj}\left(T_{wGBj}-T_{GBj}\right)-\overline{h_{ij}}S_{ij}L_{Bj}\left(T_{GBj}-T_{LBj}\right)=A R_{GBj}\frac{d}{dt}\left(\rho_{Gj}\hat{u}_{GBj}L_{Bj}\right)+\dot{m}_{Gyj}\,i_{Gyj}-\dot{m}_{Gxj-1}\,i_{Gxj-1} \quad (8)$$

where $\dot{m}_{Gxj} = \rho_{GBj}A(1\text{-}R_{LSj})|U_{GSj} - dx_j/dt|$, $\dot{m}_{Gyj} = \rho_{GBj}A(1\text{-}R_{LSj})|U_{GSj} - dy_j/dt|$.

It can be observed that Eqs. (7) and (8) have one additional term in the heat rate for the liquid film and the elongated bubble. As the liquid and the gas have different temperatures, these two phases will exchange an amount of heat in the interface region. Energy must be conserved, so the heat gained by one phase, is lost by the other, which is why the signals are opposite.

If the fluids are considered as incompressible liquid and ideal gas, the specific internal energy and enthalpy can be calculated as a function of the temperature with constants specific heats (Moran and Shappiro, 2006). Thus, it can be written:

$$\hat{u}_L = i_L = C_L T_L \qquad i_G = Cp_G T_G \qquad \hat{u}_G = Cv_G T_G \tag{9}$$

where C_L is the specific heat of the liquid, Cp_G is the specific heat at constant pressure and Cv_G is the specific heat at constant volume.

According to Kim and Ghajar (2006), Deshpande et al (1998) and others, the heat transfer in two-phase flows is influenced mainly by the liquid phase. Because of this, the equation system for the temperatures is build with the Eqs. (6) and (7) for the liquid slug and film respectively. In addition, variations of temperatures along one control volume can not be ignored. The temperature of the slug and film are calculated as the arithmetic mean of the temperatures at the control surfaces:

$$T_{LSj} = \left(T_{Lxj} + T_{Lyj}\right)/2 \quad ; \quad T_{LBj} = \left(T_{Lyj} + T_{Lxj-1}\right)/2 \tag{10}$$

For the discretization of Eqs. (6) and (7), expressions in (10) are used and it is considered an implicit scheme. The equation system is built having as its variables the temperatures T_{Lxj} and T_{Lyj}. Substituting Eq. (10) in Eqs. (6) and , applying the discretization scheme and isolating the terms in the actual instant, it is obtained Eqs. (11) and (12). The coefficients *CTF* and *CTS* are calculated according to table.

$$\left[CTF_{xj-1}\right]T^N_{Lxj-1} + \left[CTF_{yj}\right]T^N_{Lyj} = \overline{h^G_{LBj}} S_{LBj} L_{Bj} T_{wLSj} + QI + \frac{\rho_L A C_L R_{LBj} L_{Bj}}{2\Delta t}\left(T^O_{Lxj-1} + T^O_{Lyj}\right) \tag{11}$$

$$\left[CTS_{yj}\right]T^N_{Lyj} + \left[CTS_{xj}\right]T^N_{Lxj} = \overline{h^G_{LSj}} S_{LSj} L_{Sj} T_{wLSj} + \frac{\rho_L A C_L R_{LSj} L_{Sj}}{2\Delta t}\left(T^O_{Lyj} + T^O_{Lxj}\right) \tag{12}$$

Table 1. Coefficients in the discretization of the temperature system.

Coefficients	
$CTF_{xj-1} = \frac{\rho_L A C_L R_{LBj}\left(2L^N_{Bj} - L^O_{Bj}\right)}{2\Delta t} - \dot{m}_{Lxj-1} C_L + \frac{\overline{h^G_{LBj}} S_{LBj} L_{Bj}}{2}$	$CTF_{yj} = \frac{\rho_L A C_L R_{LBj} L_{Bj}}{2\Delta t} + \dot{m}_{Lyj} C_L + \frac{\overline{h^G_{LBj}} S_{LBj} L_{Bj}}{2}$
$CTS_{yj} = \frac{\rho_L A C_L R_{LSj}\left(2L^N_{Sj} - L^O_{Sj}\right)}{2\Delta t} - \dot{m}_{Lyj} C_L + \frac{\overline{h^G_{LSj}} S_{LSj} L_{Sj}}{2}$	$CTS_{xj} = \frac{\rho_L A C_L R_{LSj} L_{Sj}}{2\Delta t} + \dot{m}_{Lxj} C_L + \frac{\overline{h^G_{LSj}} S_{LSj} L_{Sj}}{2}$
$QI_j = \overline{h_{ij}} S_{ij} L_{Bj}\left(T^O_{GBj} - \frac{T^O_{Lxj-1} + T^O_{Lyj}}{2}\right)$	

Eqs. (11) and (12) constitute a second equation system for the temperatures. It strongly depends of the hydrodynamic parameters which is why its solution is found after the pressure-velocity system. The calculation of the gas temperature is performed after the solution of the temperatures system. Its solution is obtained through the discretization of Eq. (8)after the proper re-arrangement:

$$T^N_{GBj} = \frac{\overline{h^G_{GBj}} S_{GBj} L_{Bj} T_{wGBj} - QI - Cp_G\left[\dot{m}_{Gyj} T^N_{Lyj} - \dot{m}_{Gxj-1} T^N_{Lxj-1}\right] + Cv_G A R_{GBj}\left(2L^N_{Bj} - L^O_{Bj}\right)\left(\rho_{GBj}\frac{T^O_{GBj}}{\Delta t}\right)}{\overline{h^G_{GBj}} S_{GBj} L_{Bj} + Cv_G A R_{GBj}\left(2L^N_{Bj} - L^O_{Bj}\right)\left(\rho_{GBj}\frac{1}{\Delta t} + \frac{d\rho_{GBj}}{dt}\right)} \tag{13}$$

4. AUXILIARY RELATIONSHIPS

Velocity of the elongated and disperse bubbles

The first auxiliary relationship is used to calculate the velocity of the front of the bubble, calculated as the translational velocity of an elongated bubble. This velocity is described as the superposition of three effects: the mixture velocity plus the drift velocity (Nicklin et al., 1962) affected by a wake effect coefficient h related to the interaction between bubbles.

$$\frac{dy_j}{dt} = U_{Tj} = \left(c_0 J + c_1\sqrt{gD}\right)\left(1+\hbar\right) \tag{14}$$

where the coefficients c_0 and c_1 can be obtained from Bendiksen (1984). According to Bendiksen (1984), the coefficients depend of the Froude number: for Fr > 3.5: c_0 = 1.2 and c_1 = 0.0 and for Fr < 3.5: c_0 = 1.05 and c_1 = 0.54. The wake effect coefficient is calculated through the expression $\hbar = a_w exp(-b_w L_S/D)$. Rodrigues (2009) proposed using a_w = 0.4 and b_w = 1.0 for horizontal pipes.

The velocity of the back of the bubble is calculated through the mass balance in the bubble region performed by Rodrigues (2009) and modified adding the effects of the expansion due to temperature variations.

$$\frac{dx_{j-1}}{dt} = \frac{R_{GSj}U_{GSj} - R_{GSj-1}U_{GSj-1} + \left(\frac{1}{P_{GBj}}\frac{dP_{GBj}}{dt} - \frac{1}{T_{GBj}}\frac{dT_{GBj}}{dt}\right)\left(L_{Bj}R_{GBj} + \frac{L_{Sj}R_{GSj}}{2} + \frac{L_{Sj-1}R_{GSj-1}}{2}\right) + \left(R_{GBj} - R_{GSj}\right)\frac{dy_j}{dt}}{R_{GBj} - R_{GBj-1}} \tag{15}$$

Eqs. (14) and (15) determine the displacement of the unit cell along the pipe at each time step. Other constitutive equation is needed for the velocity of the dispersed bubbles (U_{GS}). However, as the flow is horizontal, it can be considered that the dispersed bubbles move with the velocity of the liquid, so $U_{GSj} = U_{LSj}$ and $U_{DSj} = 0$.

Heat transfer coefficient

As presented before, the duct is surrounded by an external flow. For the heat transfer coefficient, it must be considered the external convection, the conduction in the duct thickness and the internal convection between the duct wall and the two-phase mixture. Thus, it is used the concept of global heat transfer coefficient, based on thermal resistances (Incropera et al, 2008)

$$\frac{1}{\overline{\overline{h_\phi^G}}} = \frac{1}{\overline{\overline{h_\phi}}} + \frac{D}{2k_c} Ln\frac{D_0}{D} + \frac{D}{D_0\overline{\overline{h_0}}} \tag{16}$$

where k_c is the thermal conductivity of the pipe material, D_0 is the external diameter, h_0 is the convective coefficient of the external flow and h_ϕ is the heat transfer coefficient for each component of the unit cell which is calculated as a single-phase coefficient. According to the experimental studies of Lima (2009), the expression that better adjusts to the one-phase flow behavior is the Gnielinski correlation:

$$\overline{h_\phi} = \frac{\left(f_\phi/8\right)\left(\mathrm{Re}_\phi - 1000\right)\mathrm{Pr}_\phi}{1+12.7\left(f_\phi/8\right)^{0.5}\left(\mathrm{Pr}_\phi^{2/3}-1\right)}\frac{k_\phi}{D_\phi} \quad ; \quad f_\phi = \left[0.079\cdot Ln\left(\mathrm{Re}_\phi\right) - 1.64\right]^{-2} \tag{17}$$

This correlation has a high dependence of the Reynolds number Re_ϕ and the Prandtl Pr_ϕ number. According to Bejan (1995), the friction factor has considerable influence on the heat transfer coefficient, so that the explicit dependence in the Gnielinski correlation causes a better adjustment to the experimental data. In the case of the liquid slug, the higher turbulence occurring in this region needs to be reflected in the model, so the heat transfer coefficient h_S is increased by 30% (França et al., 2008).

Two-phase heat transfer coefficient

For the calculation of the two-phase heat transfer coefficient, the expression is based on the mechanistic model developed by França et al. (2008). The mean convective heat transfer coefficient is defined by an averaging process:

$$\overline{h_{TP}} = \frac{\int_{-L_S}^{L_B} q''S dx}{\int_{-L_S}^{L_B}\left(T_w - T\right)S dx} \tag{18}$$

where q'' is the heat flux provided to the unit cell.

The heat flux can be expressed as a function of the local heat transfer coefficients and the temperatures calculated from the energy balance. For the temperature difference between the fluid and the wall, it is considered just the liquid phase, as it is the predominant due to its higher thermal capacity. An expression is found for the two-phase heat transfer coefficient:

$$\overline{h_{TPj}} = \frac{\overline{h_{LSj}} L_{Sj}\left(T_{wiLSj} - T_{LSj}\right) + \dfrac{\overline{h_{LBj}} S_{LBj} L_{Bj}\left(T_{wiLBj} - T_{LBj}\right) + \overline{h_{GBj}} S_{GBj} L_{Bj}\left(T_{wiGBj} - T_{GBj}\right)}{\pi D}}{L_{Sj}\left(T_{wiLSj} - T_{LSj}\right) + L_{Bj}\left(T_{wiLBj} - T_{LBj}\right)} \tag{19}$$

where the numerator represents the amount of heat provided to the fluid in the unit cell and the denominator represents the mean difference between the temperatures in the wall and in the fluid. The wall temperature can be calculated assuming that all the heat provided to the wall is transferred to the fluid in the radial direction only:

$$T_{w\phi} = T_\phi - \frac{\overline{h_\phi^G} D}{\overline{h_\phi} D_0}\left(T_\phi - T_0\right) \tag{20}$$

Mixture temperature

The temperatures obtained from the heat transfer model represent the local temperature of each component of the unit cell. In order to merge all these temperatures in one that represent the entire unit cell, it will be defined the mixture temperature. This temperature is evaluated using the total energy in the entire unit cell:

$$\dot{E}_U = \dot{m} C T_m = \dot{m}_{LS}\, C_L T_{LS} + \dot{m}_{LB}\, C_L T_{LB} + \dot{m}_{GS}\, Cp_G T_{GS} + \dot{m}_{GB}\, Cp_G T_{GB} \tag{21}$$

where $\dot{E}_U$ is the total energy of the unit cell, T_m is the mixture temperature.

Eq. (21) shows that the energy of the unit cell is the sum of the energies of its components. As the gas has a low density compared to the liquid, this phase is neglected and just the liquid phase is considered. The mass flow rates are found through the velocities in each region. Therefore, the mixture temperature can be calculated using the following relationship:

$$T_{mj} = \frac{U_{LSj} R_{LSj} T_{LSj} + U_{LBj} R_{LBj} T_{LBj}}{U_{LSj} R_{LSj} + U_{LBj} R_{LBj}} \tag{22}$$

5. SOLUTION METHODOLOGY

In the previous sections, two linear equation systems were found as the result of the discretization process. The first one is used to calculate the pressure of the bubble and the velocity of the liquid slug. The second one solves the temperatures. These two systems will be solved in sequence for each time step.

In the case of the pressure-velocity system, a couple of two equations are written for each j unit cell according to Eqs. (3) and (4) ($1 \le j \le n$). If n is the number of unit cells inside the pipe, there would be $2n$ equations. That way, there is an equation system in terms of the mean velocity in the liquid slug region U_{LSj} and the pressure inside the j^{th} bubble P_{GBj}. In the case of the temperatures system, there are also two equations for each j unit cell, but the variables are T_{Lxj} and T_{Lyj} according to Eqs. (11) and (12). The set of unit cells produces two linear systems and each of them can be written as $A.Ø = B$, where $Ø$ is the unknown vector and B the source term vector. A, is a tridiagonal matrix in the pressure-velocity system and a lower bidiagonal matrix in the temperatures system. One system is solved in each time step.

The TDMA method is used to solve the pressure-velocity equation system. For the application of this method, two boundary conditions must be known for the first and last cells. In the last cell ($j = n$), it is used the value P_{GBn+1}, which represents the pressure at the exit. Commonly, the atmospheric pressure written as $P_{GBn+1} = P_{atm}$, is used at the exit. In the first cell (j = 1), it is used the value U_{LS0}, which represents the instantaneous velocity of the liquid in the first slug: $U_{LS0} = j_L + j_G$, where j_L and j_G are the superficial velocities of the liquid and gas at the entrance. For the temperature system, which has a lower bidiagonal matrix, just one boundary condition is required. Thus, it is assumed that the temperature at the entrance is known, so $T_{Lx0} = T_{en}$. A representation of the boundary conditions can be observed in Figure 2.

In order to initialize the simulation, conditions at $t=0$ must be established. In the present work, it is considered that the pipe is full of liquid with initial velocity U_{LS0} and the first bubble is positioned in $x=0$, as observed in Figure 2. The bubble and slug lengths, the superficial velocities and the volume fractions R_{GB} and R_{LS} are considered as input values. They are required whenever a new unit cell needs to be inserted at the pipe entrance. When the simulation starts (at $t=0$), two unit cell are required from the entrance conditions. The first has its bubble nose at z = 0 and the second is behind the first one still outside the pipe. One time step later, the parameters of the first unit cell are updated through the solution of the pressure-velocity system, the auxiliary relationships and the temperature system. Time steps are increased and equation systems are solved until the first bubble is completely inside the pipe. At that moment, the second bubble starts entering the pipe and a third unit cell from the entrance conditions is required. This third unit cell is positioned behind the second. This procedure is repeated for every single unit cell entering the pipe. Simulation finishes when a number of unit cells specified by the user leaves the pipe.

The lagrangian slug tracking model presented is implemented in an object-oriented computational program written in FORTRAN language, using Intel Visual Fortran as compiler. In this approach, bubbles and slugs are discrete objects which are propagated along the pipe through the governing equations. The algorithm used by the program is as follows:

1. Lecture of the input parameters: superficial velocities, fluid properties, unit cell at the entrance (L_B, L_S, R_{GB}, R_{LS}), pressure at the exit, temperature at the entrance.
2. Establishment of the initial conditions.
3. Solution of the pressure-velocity system for the n unit cells inside the pipe with Eqs. (3) and (4).
4. Calculation of velocities of the front and back of the bubble according to Eqs. (14) and (15).
5. Solution of the temperature system using Eqs. (11) and (12). Calculation of the mixture temperature and two-phase heat transfer coefficient.
6. The displacement of the unit cell is calculated by: $y_j^N = y_j^O + U_{Tj}\Delta t$ and $x_{j-1}^N = x_{j-1}^O + \left(dx_{j-1}/dt\right)\Delta t$. Parameters in the new instant turn to old.
7. Verification of entrance or exit of bubbles in the tube.
8. If the number of bubbles that leaves the tube is more than 200, simulation finishes, otherwise steps 3 to 7 are repeated.

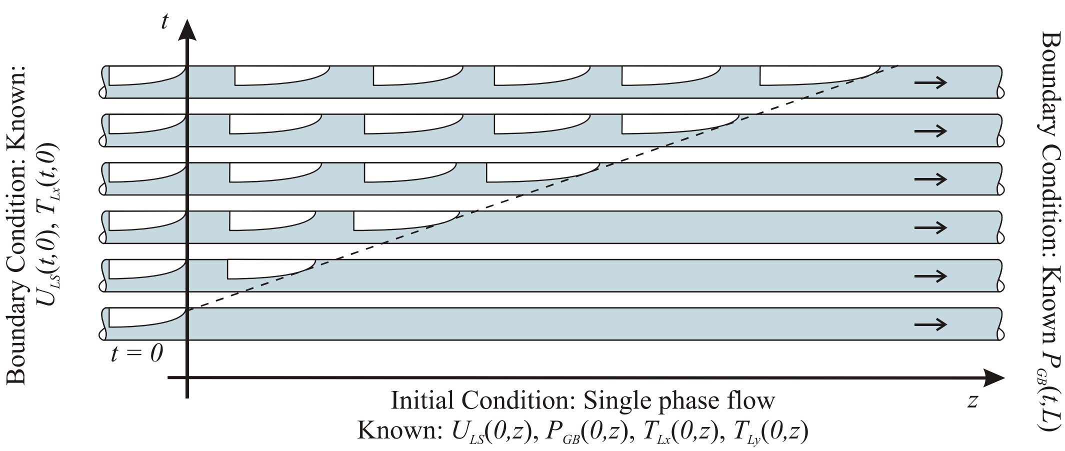

Figure 2. Representation of the boundary and initial conditions.

6. RESULTS AND DISCUSSION

The proposed model is compared with the experimental data obtained by Lima (2009). The experiments were carried out with an air-water hot mixture flowing in a 52-mm-ID copper pipe (54 mm-OD). The two-phase flow was cooled by cold water which flow co-currently in the outside annulus with a known flow rate. The 6 meter-length test section is followed by a glass window that allows flow visualization, so that, the slug and bubble length can be measured. In this experiment, Lima (2009) measured the mixture temperature at the entrance and at the exit and the two-phase heat transfer coefficient.

The external heat transfer coefficient h_0 is estimated with the Gnielinski (1976) correlation based on the cold water mean velocity and the hydraulic diameter of the annulus. The external temperature is calculated as the average temperature of the external flow at the entrance and the exit of the test section. The heat transfer coefficient in the interface h_i is considered equal to the gas heat transfer coefficient h_{GB}.

As specified before, some slug flow parameters need to be known in order to start the simulation. In this test, the superficial velocities at the entrance j_L = 1.378 m/s and j_G = 0.283 m/s, the bubble and slug length L_B = 0.34 m and L_S = 0.82 m and the volume fractions R_{GB} = 0.423 and R_{LS} = 0.97. In addition, the pressure at the exit P = 171 kPa, the temperature at the entrance T_{en} = 307.7 K, the temperature of the external flow T_0 = 284.85 K and the external coefficient h_0 = 2463 w/m²K.

Figure 3 shows the temperatures behavior along the pipe from a lagrangian probe. This type of probe tracks a determined unit-cell, and captures all its properties along its path. The thick continuous line designates the mixture temperature T_m, and the thin continuous line represents the temperature of the gas elongated bubble T_{GB}. The thick interrupted line represents the wall temperature in contact with the liquid T_{wL} and the thin interrupted line represents the wall temperature in contact with the gas elongated bubble T_{wGB}. It is noticeable the large differences between the liquid and the gas temperatures, evidencing the existence of heat exchange between the phases in the bubble region. As the walls are nearby the external flow, their temperatures are closer to the external temperature T_0. However, they show the same tendency as the phases they are in contact with, but differing in a constant displacement.

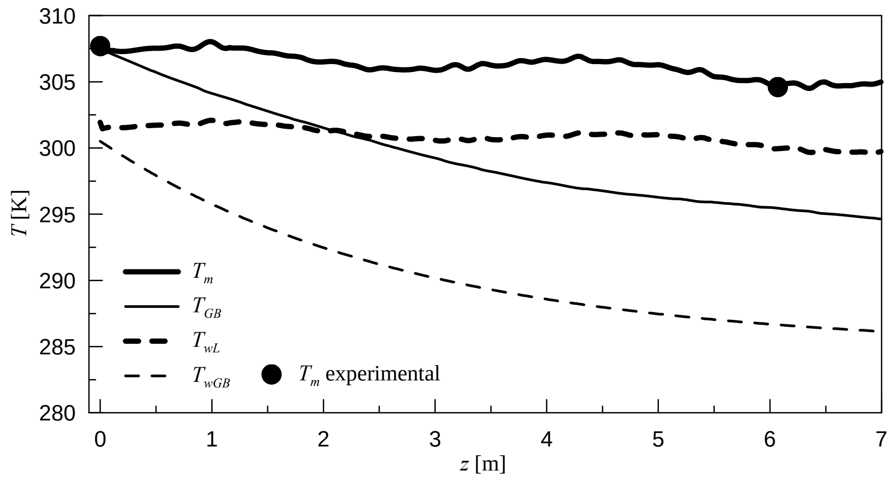

Figure 3. Temperatures along the pipe extension.

It can be observed that there is a good agreement between the simulated and the experimental value for the mixture temperature, evidencing the consistence of the model. As expected, the liquid phase shows lower variations compared to the temperature of the elongated bubble due to its higher specific heat. Thus, the exponential trend of the constant temperature distributions is more evident in the gas.

The distribution for the mixture temperature along the pipe in Figure 4A presents some oscillations. These oscillations are product of the spatial resolution of the slug tracking model, as the control volumes used are in the integral form. In spite of the oscillations, the results show the same tendency as the experimental values.

Figure 4 shows some parameters of slug flow along the pipe from the lagrangian probe. The two-phase heat transfer coefficient h_{TP} can be evaluated at any position of the pipe through Eq. (19). In Figure 4a, this value is compared to the experimental reported by Lima (2009) and considering the error (21%), the agreement obtained is good. It can be observed that despite the temperature variation along the pipe, the heat transfer coefficient is not affected significantly, so it can be considered an average value for the whole simulation.

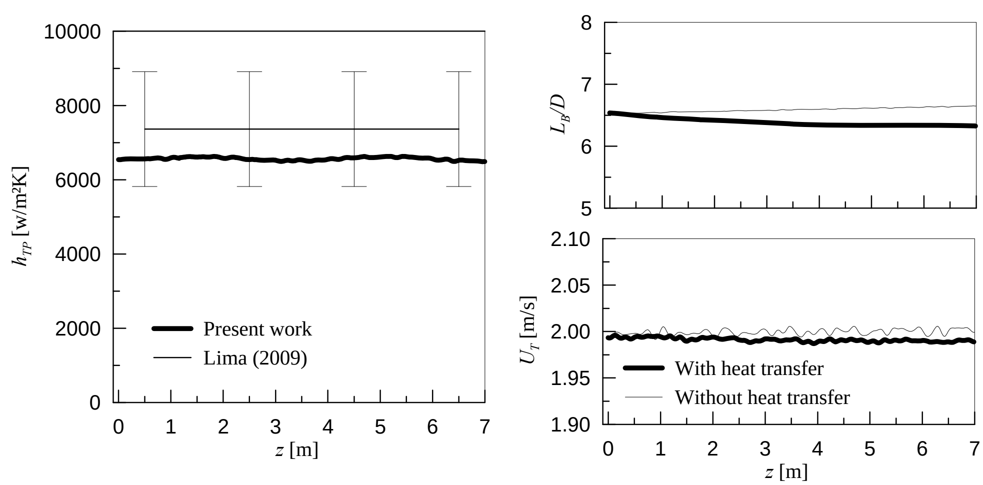

Figure 4. Parameters along the pipe.

As observed in Eq. (1) and (15), the heat transfer and the temperature variations affect the hydrodynamic parameters. Figure 4b-c are presented to evidence that the model represents correctly the effects of the gas expansion due to temperature variations in an ideal gas. The thick line designates the results with the heat transfer term and the thin line presents the same results when heat transfer terms are omitted.

Figure 4b shows the evolution of the bubble length along the pipe extension. Omitting the heat transfer terms causes the bubble to expand due to pressure drop which is clearly represented in the thin line. When heat transfer is considered, there is a conflict because the bubble will expand due to pressure drop but it will also compress because of the cooling. In Figure 4b it is shown that in spite of the temperature variation being little, it has a bigger impact than the pressure. However, as the temperature gradient declines far from the entrance (Figure 3), the expansion due to pressure is compensated with the compression due to temperature, maintaining a constant length near the exit.

Figure 4c presents the translational velocity of the elongated bubble U_T along its path in the pipe. As observed in Eq.(14), the U_T velocity depends of the mixture velocity, which also varies with the expansion of the bubble, as the superficial velocity of the gas j_G depends of the occupied volume. Just as the bubble length, the translational velocity suffers a little decline due to the compression caused by cooling.

Lima presented 24 more tests with different combinations of air-water superficial velocities where the two-phase heat transfer coefficient was calculated through the temperatures measured. Liquid superficial velocities are ranged from 0.579 to 1.380 m/s and gas superficial velocities are ranged from 0.217 to 0.795 m/s. For this set of experiments, there were no data for the entrance unit-cell (L_B, L_S, R_{GB} and R_{LS}), so these parameters had to be estimated. It was used the methodology proposed by Perea (2011) where the unit cell was generated through the Taitel and Barnea (1990) model.

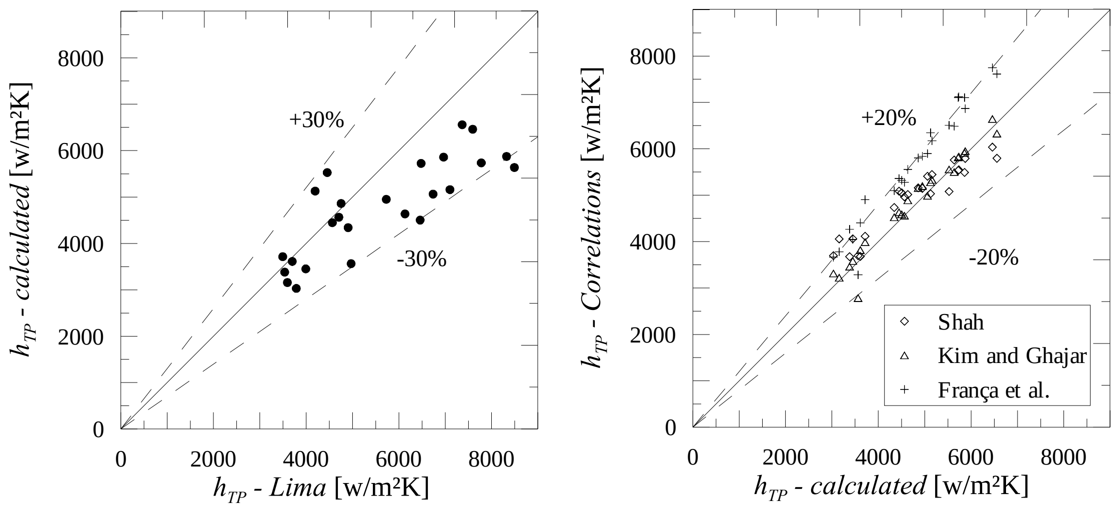

Figure 5. Two-phase heat transfer coefficient for the Lima (2009) experiments.

Figure 5a shows the comparisons between model predictions and experimental measurements of the two-phase heat transfer coefficients for the 25 experiments. It can be observed that the predicted values agree with the experimental measurements quite well. Most of the data points are located inside the ±30% error band, observing that the model tends to underestimate. However, as the experimental measurements have an average experimental error of 20%, a prediction with 30% error band is quite good. The discordance may have been caused by the overestimation of the bubble length, as it was calculated. As observed in Eq.(19), the h_{TP} is weighted with the film (or bubble) and slug lengths. As the liquid film has lower velocity then the slug, its h_{LB} will be smaller, so an oversized bubble will reduce the real value of h_{TP}.

Figure 5b compares the results for the predicted h_{TP} with other correlations on the literature. The Shah (1981) correlation shows good agreement with the mechanistic model with a 15% of error range. However, this correlation considers neither the flow pattern nor the effective wet perimeter, as it only depends on the superficial velocities, so probably it does not reproduce heat transfer entirely.

The proposed model shows an excellent agreement with the Kim and Ghajar (2006) correlation, with a 10% error range. This correlation is apparently independent of the flow pattern; however, it considers it through the introduction of a flow pattern factor. This flow pattern factor quantifies the effective wet perimeter through an approximate volume fraction. As the model proposed depends of the bubble and slug lengths, the agreement with the correlation is good.

For the França et al. (2008) correlation, good agreement is found, as all the calculated data are confined in the ±20% error band. This fact is based on the similarity that the expression (19) has with the one that comes from the mechanistic model of França et al. (2008). However, differences are evident as Eq. (19) considers the temperature difference between the fluid and the wall. França et al. (2008) regards this temperature difference as constant for both fluids, however, as shown in Figure 3 this difference is not uniform due to the higher thermal capacity of the liquid.

7. CONCLUSIONS

Numerical simulation of non-boiling heat transfer in two-phase slug flow was presented. The slug tracking model presented by Rodrigues (2009) was modified to consider the gas compressibility due to pressure and temperature variations. Then, energy balance in unsteady regime was performed to obtain a model function of the temperatures. The governing equations of the heat transfer were coupled with the slug tracking model and discretized properly. As a result of the discretization, two equation systems are obtained: one from the slug tracking model that solves the slug velocity and the bubble pressure, and one from the energy balance that solves the temperatures.

Simulations results show that the model captures the temperature intermittency of the flow. It is evidenced that the temperature of the liquid has noticeable differences with the gas, which is why the heat exchanged between the two phases in the interface should not be neglected. Temperature variation affects two slug flow parameters mainly: the bubble length and the translational velocity, both variations caused by the gas compressibility. The expression proposed for the two-phase heat transfer coefficient presented good agreement with the experimental data, although it tends to underestimate it. Agreement with correlations from the literature is even better.

8. REFERENCES

Barnea and D., Taitel, Y., 1993 “A Model for Slug Length Distribution in Gas – Liquid Slug Flow”, International Journal of Multiphase Flow, Vol. 19, No. 5, pp. 829-838.

Bendiksen, K., 1984 “An Experimental Investigation of the Motion of Long Bubbles in Inclined Tubes”. International Journal of Multiphase Flow, Vol. 10, No. 4, pp. 467-483.

Dukler A. E. e Hubbard M. G., 1975, “A model for gas-liquid slug flow in horizontal and near horizontal tubes”. Ind. Eng. Chem. Fundam., 14 (4), pp. 337-347.

França, F., Bannwart, A. C., Camargo, R. M. T., Gonçalves, M., 2008, “Mechanistic Modeling of the Convective Heat Transfer Coefficient in Gas-Liquid Intermittent Flows”, Heat Transfer Engineering, 29(12) pp. 984-998.

Gnielinski, V., 1976, “New equations for heat and mass transfer in turbulent pipe and channel flow” International Chemical Engineering, Vol. 16, No. 2, 359-368.

Hetsroni, G., Hu, B., Yi, J., Mosyak, A., Yarin, L., Ziskind, G., 1998, “Heat transfer in intermittent air-water flows – Part I” International Journal of Multiphase Flow, Vol. 24, No. 2, pp. 165-188.

Incropera, F., DeWitt, D., Bergman, T., Lavine, A., 2008, “Fundamentos de Transferência de Calor e de Massa”, 6a Ed., Livros Técnicos e Científicos Editora S.A.

Kim, J. and Ghajar, A., 2006, “A general heat transfer correlation for non-boiling gas-liquid flow with different flow patterns in horizontal pipes”, International Journal of Multiphase flow 32, pp 447-465.

Lima, I. N. R. C., 2009, “Estudo Experimental da Transferência de Calor no Escoamento Bifásico Intermitente Horizontal” São Paulo: Universidade Estadual de Campinas, Brazil, Master Thesis 135 p.

Moran, M. e Shapiro, H., 2006, “Fundamentals of Engineering Thermodynamics”, 5th Ed. John Wiley & Sons, Inc.

Nydal, O. J., Banerjee, S., 1995 “Dynamic Slug Tracking Simulations for Gas-Liquid Flow in Pipelines”. University of California Santa Barbara, United States.

Patankar, S.V., 1980, “Numerical Heat Transfer and Fluid Flow”. Philadelphia: Taylor & Francis.

Rodrigues, H. T.,2009 “Simulação Numérica de Escoamento Bifásico gas-líquido no padrão de golfadas utilizando um modelo lagrangeano de seguimento de pistões”. Universidade Tecnológica Federal do Paraná. Curitiba, Brasil, pp. 192 Master thesis.

Shah, M., 1981, “Generalized prediction of heat transfer during two-component gas-liquid flow in tubes and other channels” AIChE Sympossium Series Vol. 77, No. 207, pp. 140-151.

Shoham, O., 2006, “Mechanistic Modeling of Gas-Liquid Two-phase Flow In Pipes” Society of Petroleum Engineers, Richardson, TX, 396p.

Taitel, Y. and Barnea, D., 1990, "Two phase slug flow", Advances in Heat Transfer, Hartnett J.P. and Irvine Jr. T.F. ed., vol. 20, 83-132, Academic Press.

9. RESPONSIBILITY NOTICE

The authors are the only responsible for the printed material included in this paper.